

Searching for the Physical Driver of the Correlations for an X-ray Selected AGN Sample

Da-Wei Xu¹*, S. Komossa² and Jian-Yan Wei¹

¹ National Astronomical Observatories, Chinese Academy of Sciences, Beijing 100012, China

² Max-Planck-Institut für extraterrestrische Physik, Postfach 1312, D-85741 Garching, Germany

Abstract Direct correlation analysis is presented for a sample of 155 low-redshift bright X-ray selected ROSAT Seyfert 1 type AGN. We confirm the well-known relations between the strengths of Fe II, [O III] emission and the X-ray slope. We also detect striking correlations between H β redshift (or blueshift), flux ratios of Fe II to H β broad component. The physical driver of these correlations is most likely the Eddington ratio.

Key words: Galaxies: Seyfert – Quasars: emission lines – X-rays: galaxies

1 INTRODUCTION

In the course of the ROSAT All Sky Survey (RASS) (Voges et al. 1999), many new AGN have been identified by different teams, confirming that X-ray surveys are very efficient in finding new AGN. Multi-wavelength observations of well-defined source samples have proved an effective means in understanding the physical processes in AGN.

In the last decade, several correlations between optical emission line properties and X-ray properties were noted (Boroson & Green 1992, Lawrence et al. 1997, Grupe et al. 1999, Vaughan et al. 2001). For instance, the strong correlations between optical Fe II, [O III] λ 5007 line strengths, velocity width of H β and the slope of soft X-ray continuum (α_X). These correlations received great interest previously and were expected to give important insight into the AGN phenomenon. Still, however, their interpretation remained unclear. It is therefore of great importance to test whether these correlations are fundamental properties or subtle selection effects, and search for new ones. A large and homogeneous X-ray selected AGN sample is therefore of great importance in studying the correlations between the optical to soft X-ray continuum and optical emission line properties of AGN.

We have studied the emission line and continuum properties of a sample of 155 bright X-ray selected ROSAT Seyfert 1 type AGN. In this paper, we present the statistical analysis of the sample. Luminosities are calculated assuming a Hubble constant of $H_0 = 50 \text{ km s}^{-1} \text{ Mpc}^{-1}$ and a deceleration parameter of $q_0 = 0$.

* E-mail: dwxu@bao.ac.cn

2 SAMPLE SELECTION

The X-ray sources with the highest X-ray-to-optical flux ratio are: BL Lac objects, emission line AGN, clusters of galaxies etc. However, X-ray flux is difficult to evaluate before optical identification. According to our statistical analysis of known RASS bright source catalog (RASS-BSC, Voges et al. 1999) X-ray sources, we found that there is an apparent gap between Galactic stars and extragalactic objects. As can be seen in Fig. 1, 92% AGN concentrate in the region: $\log C \geq -0.4 R + 4.9$. Thus, choosing $\log C \geq -0.4 R + 4.9$ is expected to be efficient for the preselecting of AGN and can avoid too many O – M stars being included in the sample.

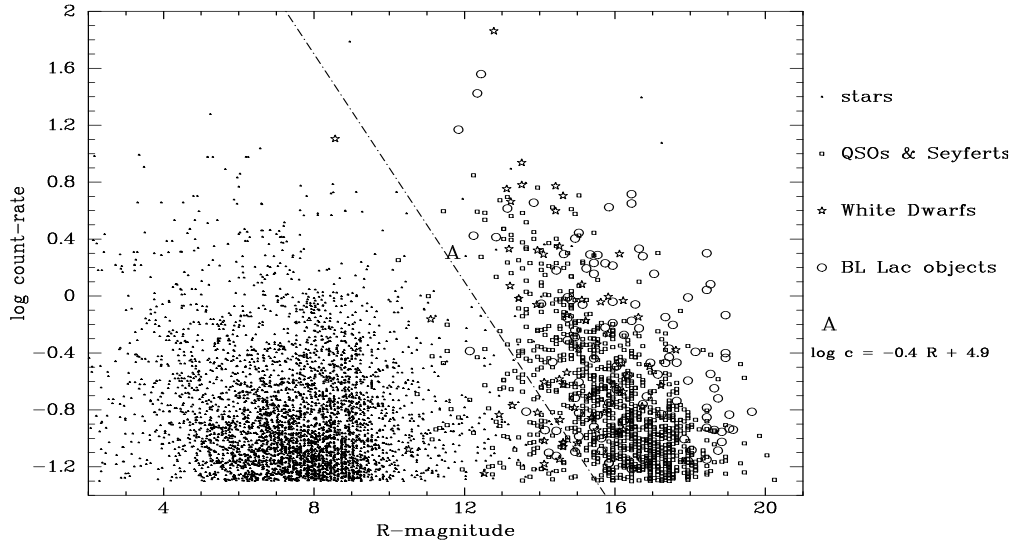


Fig. 1 Count rates as a function of R magnitudes for known sources.

Our sample of 155 Type 1 AGN results from the optical identification of the X-ray sources with high X-ray to optical flux ratio (f_X/f_{opt}) in the RASS-BSC (see Wei et al. 1999 for optical identification). Forty out of 155 sources are known AGN which meet our selection criteria. The sample was selected using the following criteria:

1. An alternative high X-ray-to-optical flux ratio criterion, i.e., $\log CR \geq -0.4 R + 4.9$, where CR and R represent X-ray count rate and R magnitude respectively.
2. Declination $\delta \geq 3^\circ$.
3. Galactic latitude $|b| \geq 20^\circ$.
4. Optical counterparts within a circle with radius $r = r_1 + 5''$, where r_1 is the RASS position error.
5. Optical counterparts with R magnitudes between 13.5 and 16.5.

3 LINE MEASUREMENTS

We adopt the method described by Boroson & Green (1992), using the Fe II template of I Zw 1 to determine the strength of the Fe II emission and carefully remove the Fe II multiplets from the optical spectra ¹.

¹ Based on data obtained with the 2.16 m telescope at Xinglong station, NAOC.

The Fe II subtracted spectra were used to measure the non-Fe II line properties. In order to isolate the broad H β component in all spectra, we have assumed that the emission line profiles can be represented by a single or a combination of Gaussian profiles. We used the IRAF package SPECFIT² to measure blended lines. The broad component of H β is referred as H β_b , and the narrow component as H β_n . For H β lines with asymmetric profile, the two Gaussian components are not stationary in wavelength.

The optical index α_{opt} was calculated using the continuum flux density at 4400Å and 7000Å in the rest frame. The X-ray spectral slope $\alpha_X (F_\nu \propto \nu^{-\alpha})$ was estimated using the ROSAT hardness ratios HR1 and HR2 from RASS-BSC.

The full derived parameters were listed in Xu et al. (2003).

4 CORRELATION ANALYSIS

We explore whether the various emission-line and continuum properties correlate with one another. For this purpose, we calculated the Spearman rank-order correlation matrix, along with its significance matrix for measured properties. The complete correlation coefficient matrix is shown in Table 1. The probability of the null correlation, Ps, for a sample with corresponding correlation coefficient Rs is also given in Table 1 for entries with Ps < 0.01. A set of 12 different properties results in 66 correlation coefficients. Among them, 31 correlations were found with two-sided probabilities Ps < 0.01. Four are due to the dependent parameters, e.g., relative strength of Fe II to H β and Fe II EW; 12 are degenerate correlations, i.e., different measures of the same property (e.g., [O III] EW, [O III]/H β_b and [O III]/H β_n) all correlate with another property (e.g., Fe II EW); and therefore 15 are independent correlations at the > 99% confidence level.

Table 1 Spearman Rank-Order Correlation Coefficient Matrix

Property	(1)	(2)	(3)	(4)	(5)	(6)	(7)	(8)	(9)	(10)	(11)	(12)
(1) FWHM(H β_b)	-	0.002	0.032	-0.32 (0.0020)	0.35 (0.0009)	-0.59 (0.0000)	-0.05	0.34 (0.001)	-0.20	-0.04	0.38 (0.0003)	0.48 (0.0000)
(2) FWHM(H β_n)	-	0.46 (0.0000)	0.30 (0.004)	-0.263 (0.004)	0.23	-0.294 (0.005)	-0.15	0.23	-0.104	-0.66 (0.0000)	0.11	
(3) FWHM([OIII])	-		-0.03	0.004	-0.02	-0.08	0.02	-0.06	-0.166	-0.15	-0.01	
(4) EW FeII	-			-0.59 (0.0000)	0.81 (0.0000)	-0.546 (0.0000)	-0.471 (0.0000)	0.41 (0.0001)	-0.129	-0.544 (0.0000)	0.06	
(5) EW [OIII]	-				-0.64 (0.0000)	0.73 (0.0000)	0.33 (0.0019)	-0.39 (0.0002)	0.195	0.67 (0.0000)	0.05	
(6) FeII/H β_b	-					-0.23 (0.0000)	-0.64 (0.0011)	0.34 (0.0000)	-0.055	-0.60 (0.0000)	0.24	
(7) [OIII]/H β_b	-						0.009 (0.0017)	-0.33 (0.0000)	0.27 (0.0000)	0.45 (0.0038)	-0.314 (0.0038)	
(8) Δv^a	-							-0.24	0.147	0.375 (0.0003)	0.14	
(9) α_X	-								-0.236	-0.37 (0.0004)	0.36 (0.001)	
(10) α_{opt}	-									0.109	-0.29 (0.0069)	
(11) [OIII]/H β_n	-											0.1
(12) $\log \nu L_{250 \text{ eV}}$	-											-

^avelocity shift between broad and narrow Gaussian components of H β in units of km s⁻¹. Positive velocities refer to redshifts with respect to the narrow component velocities, whereas negative velocities indicate blueshifts.

² SPECFIT is developed and kindly provided by Dr. G. Kriss.

5 RESULTS

This paper presents a spectral analysis of a bright AGN sample selected from the RASS-BSC. The sample comprises 155 Seyfert 1 type AGN and is dominated by moderate luminosity objects ($M_B \approx -23 \pm 2$) with an average redshift $\langle z \rangle = 0.2$. The mean X-ray spectral slope of the sample is $\langle \alpha_X \rangle = 1.43$.

Our conclusions based on the correlation analysis can be succinctly summarized as follows:

- The previously reported correlations between the strengths of Fe II, [O III] emission and the X-ray slope are confirmed. Strong optical Fe II blends go along with weak forbidden emission lines (e.g., [O III]) and steep X-ray slopes.
- The anti-correlation between the X-ray spectral slope α_X and the FWHM of $H\beta$ becomes prominent as far as the high luminosity AGN are concerned.
- Striking correlations between the $H\beta$ redshift, Fe II/ $H\beta_b$ and [O III]/ $H\beta_n$ are found. Figure 2 shows the correlations. The correlations covering [O III]/ $H\beta_n$ have never been investigated by other authors so far. There is a general trend that strong Fe II/ $H\beta_b$ -weak [O III]/ $H\beta_n$ objects tend to have blueshifts in $H\beta$ while strong [O III]/ $H\beta_n$ -weak Fe II/ $H\beta_b$ objects tend to have redshifts in $H\beta$.

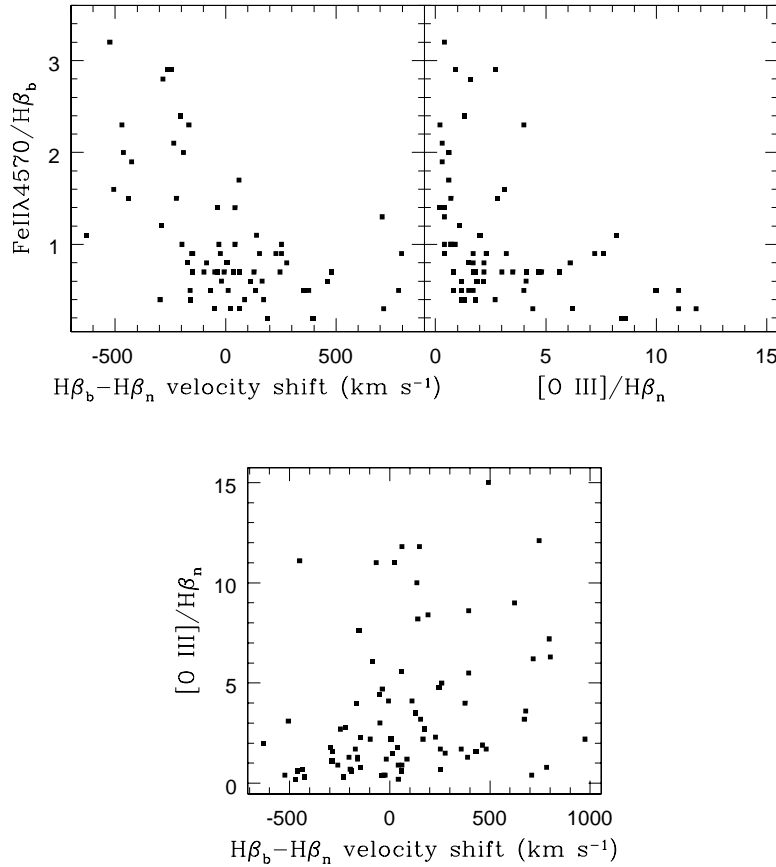


Fig. 2 Correlation diagrams for Fe II $\lambda 4570/H\beta_b$, $H\beta_b-H\beta_n$ velocity shift and [O III]/ $H\beta_n$.

6 DISCUSSION AND FUTURE WORKS

The observed trends are most likely driven by the Eddington ratio (L/L_{Edd}), which is consistent with the interpretation of the “Eigenvector 1 correlations” (Boroson & Green 1992). Accreting systems in high L/L_{Edd} AGN will drive relatively thick outflows due to their larger photon luminosities per unit gravitational mass. As the velocity of the outflow increases, $H\beta$ develops an increasing excess on the blue wing. The corresponding blue $H\beta_b$ velocity shift in comparison with [O III] can be also well predicted because both the line asymmetry and the shift of the line centroids are effects of the same process. In that case the NLR would consist of denser clouds due to the strong outflow. High-density NLR clouds would then also lead to a suppression of [O III] strength. Some suggestions have been proposed for the connection between strong Fe II emission and large L/L_{Edd} , though it is more difficult to illustrate directly, e.g., a steep X-ray spectrum coupled to a flatter EUV spectrum will lead to a thicker BLR (e.g., Komossa & Meerschweinchen 2000, Pounds et al. 1995) and thus stronger Fe II emission if the the low-excitation part of the BLR is mechanically heated.

Principle Component Analysis (PCA) is a useful tool for multivariate analysis. For a set of measured quantities, PCA defines a set of new orthogonal variables, called the principle components (PCs), which best describe the variance in the data. The great importance of the PCA is: the PCs which explains a significant fraction of the total sample variance might be related to one or more underlying fundamental physical drivers that govern the correlations between the observed parameters.

Though the observed trends of the present sample favor the L/L_{Edd} interpretation, a PCA is badly needed in order to further test the favored scenario and search for the relationship between the PCs and the physical drivers. Work on this is now in progress.

References

- Boroson T. A., Green, R. F., 1992, *ApJS*, 80, 109
Grupe D., Beuermann K., Mannheim K., Thomas H. C., 1999, *A&A*, 350, 31
Komossa S., Meerschweinchen J., 2000, *A&A*, 354, 411
Lawrence A., Elvis M., Wilkes B. J., McHardy I., Brandt N., 1997, *MNRAS*, 285, 879
Pounds K. A., Done C., Osborne J. P., 1995, *MNRAS*, 277, L5
Vaughan S., Edelson R., Warwick R. S. et al., 2001, *MNRAS*, 327, 673
Voges W., Aschenbach B., Boller Th. et al., 1999, *A&A*, 349, 389
Wei J. Y., Xu D. W., Dong X. Y., Hu J. Y., 1999, *A&A*, 139, 575
Xu D. W., Komossa S., Wei J. Y. et al., 2003, *ApJ*, 590, 73